Pseudo-oriented dipole calculations of the lattice potential and phase transition interpretation in KCN

1993 J. Phys.: Condens. Matter 5 7203

(http://iopscience.iop.org/0953-8984/5/39/008)

J. Phys.: Condens. Matter 5 (1993) 7203–7214. Printed in the UK

Pseudo-oriented dipole calculations of the lattice potential and phase transition interpretation in KCN

P Bourson and D Durand

Groupe MOPS, Centre Lorrain d'Optique et Electronique des Solides, Université de Metz-Supelec, 2 rue E Belin-Technopôle, Metz 2000, 57078 Metz Cédex 03, France

Received 17 May 1993

Abstract. Using different lattice potential calculation models, we attempt to explain the phase transition process and the evolution with the temperaure of the CN^- molecule orientation in KCN. These calculations are made for the pseudo-cubic phase and consist of a comparison between two lattice potential models, one in which a three-body interaction is introduced to take account of the anisotropic evolution with temperature of the elastic constants, and the other—a so-called 'pseudo-oriented dipole' model—in which calculations are made with CN^- elastic dipoles oriented along the principal ⟨110⟩, ⟨001⟩ and ⟨111⟩ cubic directions of the pseudo-cubic phase.

1. Introduction

At room temperature, a KCN crystal has a pseudo-cubic NaCl-type structure in which the CN^- dumbbell is rapidly reorienting between its different possible orientations ⟨001⟩, ⟨110⟩ and ⟨111⟩ [1].

As the temperature is lowered, an order–disorder phase transition appears at 168 K and a ferroelastically ordered structure is observed with an orthorhombic cell as shown in figure 1 [2].

In this phase no electrical order appears; the CN^- electric dipole lies close to the former ⟨110⟩ directions of the cubic cell and can still flip over 180°. In this elastically ordered phase, it is not possible to distinguish between C and N ions.

With decreasing temperature an electrically ordered phase appears gradually at around 80 K, also showing an orthorhombic structure with an antiferroelectric ordering of CN^- dipoles.

Similarly to KCN, other alkali cyanides undergo structure phase transitions (as summarized in [3]), revealed close to the transition by an anamolous softening of the elastic constant c_{44} [4, 5] which leads to a large Cauchy discrepancy $c_{12} - c_{44}$ [5]. This softening has to be introduced into lattice potential calculations.

In our calculations, we use a standard lattice potential model in which we introduce a three-body interaction (TBI) in the Coulomb potential as described by Cochran [6] in order to take into account the anisotropic behaviour of the evolution of the alkali-cyanide elastic constants with temperature.

In the first step, we assume that the CN^- molecule has a spherical shape. This assumption appears to be correct at high temperatures when the CN^- dumbbell is rotating rapidly (dipole reorientation rate $\tau = 10^{-13}$ s [3]). The CN^- molecule is also compact ($r_C = r_N = 1.185$ Å and the distance between C and N is small: $r_{C-N} = 1.17$ Å [7]).

0953-8984/93/397203+12$07.50

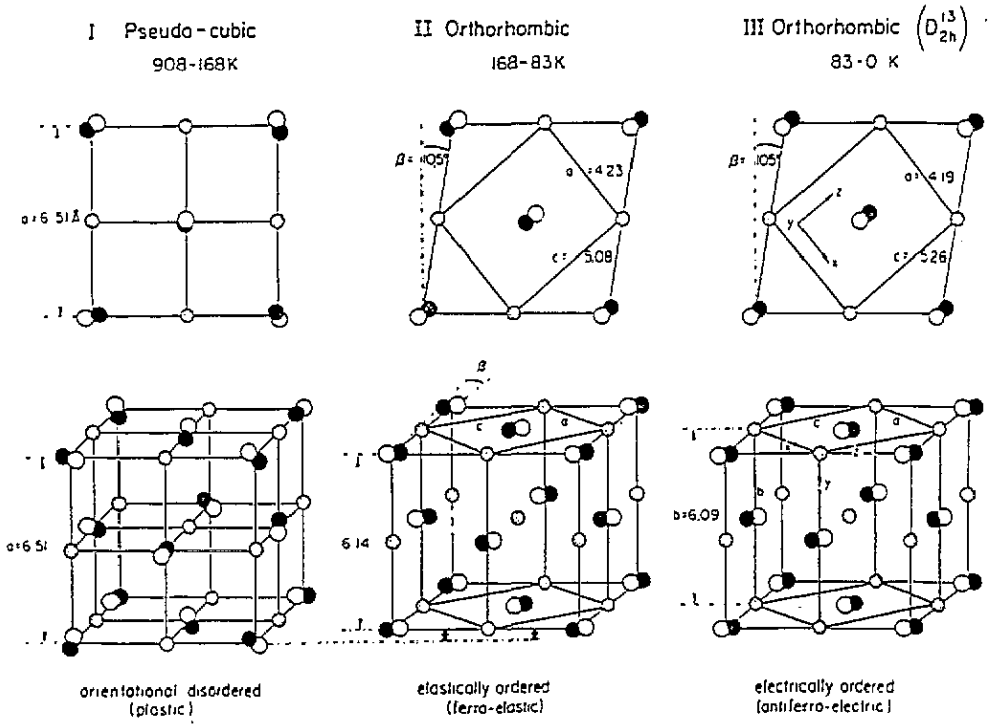

Figure 1. Structure of KCN in orientationally disordered (I), elastically ordered (II) and electrically ordered (III) phases. For the latter two, the new orthorhombic cell with axes *a*, *b* and *c* is indicated within the framework of the original cubic structure. (From Durand *et al* [2].)

In the second step, using the averaged overlap parameter found in the previous hypothesis, we calculate a new lattice potential in which the CN^- molecule is assumed to be made up of two identical ions separated by 1.17 Å [7]. This 'aspherical molecule' is oriented along the main cubic directions ⟨001⟩, ⟨110⟩ and ⟨111⟩ which are still possible with a large probability in the cubic phase [1].

The comparison between the values of potential calculated with the TBI model and with the 'pseudo-oriented-dipole' (POD) model provides a phenomenological interpretation of the phase transition process in KCN.

1.1. Rigid ion model

The standard lattice potential is calculated by evaluating the contributions of the Coulomb potential W_C, the van der Waals potential W_{VDW} and the overlap repulsive (Born–Mayer) potential W_{BM} to the energy of the lattice [8]:

$$W_L(r) = W_C(r) + W_{VDW}(r) + W_{BM}(r). \tag{1}$$

The Coulomb contribution $W_C(r)$ is given by the well known expression

$$W_C = \sum_{ij} \frac{Z_i Z_j}{r_{ij}} e^2 = -\frac{\alpha_M e^2 Z^2}{R} \tag{2}$$

where $Z = \pm 1$ for a singly charged ionic crystal, α_M is the Madelung constant and R is the nearest-neighbour separation between positive and negative ions at equilibrium (in the NaCl structure, $R = \frac{1}{2}a_0$ where a_0 is the cubic lattice parameter).

The van der Waals potential is given by the relation

$$W_{VDW}(r) = -\sum_{ij} \frac{c_{ij}}{r_{ij}^6} - \sum_{ij} \frac{d_{ij}}{r_{ij}^8} \tag{3}$$

where the c_{ij} are the dipole–dipole van der Waals coefficients, the d_{ij} are the quadrupole–dipole coefficients and r_{ij} is the distance between ions i and j. These coefficients have been evaluated (table 1) using the Slater–Kirkwood variational method [9]. They are given by

$$c_{ij} = (3eh/2\sqrt{m})\{\alpha_i\alpha_j/[(\alpha_i/N_i)^{1/2} + (\alpha_j/N_j)^{1/2}]\} \tag{4}$$

and

$$d_{ij} = (27h^2/8m)\alpha_i\alpha_j \times [(\alpha_i/N_i)^{1/2} + (\alpha_j/N_j)^{1/2}]^2/\{\alpha_i/N_i + \alpha_j/N_j + \tfrac{20}{3}[(\alpha_i/N_i)(\alpha_j/N_j)]^{1/2}\} \tag{5}$$

in which N_i and N_j are the effective numbers of electrons for the ions i and j, respectively, participating in the van der Waals interaction. α_i and α_j are the electronic polarizabilities of ions i and j, respectively.

Table 1. *van der Waals coefficients calculated by the Slater–Kirkwood equation [9].*

	c_{ij} (kcal Å^6 mol^{-1})	d_{ij} (kcal Å^8 mol^{-1})
K–K	1145.44	484.08
K–CN	2040.34	1329.42
CN–CN	4034.17	3271.60

Quantitative values for each ion are given in table 2; the N_i have been evaluated by Scott and Scheraga [10] and the electronic polarizability of K^+ ions by Tessman *et al* [11].

Table 2. Parameters used in our models: the ionic radius r in the Born model, the effective number N_i of electrons and the electric polarizability α_i.

Ion	r (Å)	N_i	α (Å^3)
K^+	1.503 [13]	17 [9]	1.33 [10]
CN^-	1.77 [7]	12 [9]	3.458

The polarizability of the CN^- dumbbell has been calculated by Gready *et al* [12] who gives values of α_{zz} for polarizability along the molecule axis and α_{xx} in the perpendicular direction.

Since we assume a spherical shape for the CN^- ion, we use in our calculation a mean polarizability for CN^- given by

$$\alpha_{CN} = \tfrac{1}{3}\alpha_{zz} + \tfrac{2}{3}\alpha_{xx}. \tag{6}$$

The short-range overlap repulsive contribution to the potential has the general expression (according to Born and Mayer [14])

$$W_{BM}(r_{ij}) = \sum_{ij} b B_{ij} \exp\left(\frac{r_i + r_j - r_{ij}}{p}\right) \tag{7}$$

where r_i and r_j are the ionic radius of ion i and j, respectively, evaluated from the Born model [8] and r_{ij} is the distance between the centres of mass of ions i and j. B_{ij} are the Pauling [15] coefficients defined by

$$B_{ij} = 1 + Z_i/n_i + Z_j/n_j \tag{8}$$

where Z_i and Z_j are the valences of ion i and j, respectively, and n_i and n_j are the numbers of outer electrons of ion i and ion j, respectively.

For the NaCl-type structure of KCN, we take into account only the first- and second-nearest-neighbour contributions ($r_{ij} = R$ and $R\sqrt{2}$).

$W_{BM}(r)$ reduces to the following expression:

$$W_{BM}(R) = b\{6B_{KCN}\exp[(r_K + r_{CN} - R)/p] + 4\exp(-R\sqrt{2}/p)[B_{KK}\exp(2r_K/p) + B_{CNCN}\exp(2r_{CNCN}/p)]\}. \tag{9}$$

In this calculation, the CN^- dumbbell is assumed to be rapidly rotating; thus a mean radius r_{CN} has been chosen as represented in figure 2.

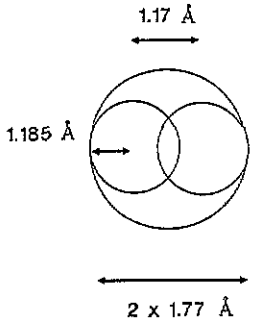

Figure 2. Illustration of the characteristic lengths for the CN^- dumbbell.

Two unknown parameters b and p are introduced into this repulsive contribution.

The parameter b represents the strength of the repulsive potential and will be determined by the equilibrium condition when the derivative of the total potential with respect to r is equal to zero at the equilibrium distance R:

$$(dW_L/dr)|_{r=R} = 0. \tag{10}$$

p represents the hardness overlap parameter. It is assumed to be the same for each neighbouring ion irrespective of its positive or negative nature. Thus p represents a mean value of the overlap. It depends on temperature and is determined using the general expression of the bulk modulus $1/K$ for the FCC structure which depends on the elastic constant values:

$$\frac{1}{K} = (1/18R)(\partial^2/\partial r^2)[W_L(r)]|_{r=R}. \tag{11}$$

1.2. Three-body interaction model

In fact, CN^- is not spherical and thus KCN presents a large elastic anisotropy before the phase transition.

This anisotropy is revealed by a large Cauchy discrepancy $c_{12} - c_{44}$, especially when approaching the phase transition where a softening of c_{44} is observed.

In order to take account of this anisotropy we introduce a three-body contribution to the total potential using the model proposed by Cochran [6].

In this model, the charge Ze of an ion is modified by the overlap interaction of neighbouring ions and becomes $Ze[1 + 6f(r)]$ in which $f(r)$ has the general expression

$$f(r) = f_0 \exp(-r/p). \tag{12}$$

p has the same meaning as before. Thus, the Coulomb potential evaluated only for the six nearest neighbours is now modified and has the general expression

$$W_C(R) = -(\alpha_M e^2 Z^2/R)[1 + 6f_0 \exp(-R/p)]^2. \tag{13}$$

In this expression the quantity $1 + 6f_0 \exp(-R/p)$ represents a charge-transfer factor between neighbouring ions.

In the NaCl-type structure, according to the work of Cochran [6], the Cauchy discrepancy and the function $f(r)$ are related by the following relation:

$$c_{12} - c_{44} = 0.1942(\partial/\partial r)[1 + 6f_0 \exp(-r/p)]^2. \tag{14}$$

It should be remarked that, in alkali halides, the Cauchy discrepancy of $c_{12} - c_{44}$ is small ($(0.1\text{–}0.01) \times 10^{11}$ dyn cm^{-2}) and the factor $[1 + 6f_0 \exp(-R/p)]^2$ is usually reduced to $1 + 12f_0 \exp(-R/p)$ [16].

For KCN, the Cauchy discrepancy is important ($(1\text{–}1.5) \times 10^{11}$ dyn cm^{-2}) and this simplification is not possible.

Knowledge of $c_{12} - c_{44}$ at each temperature gives a relation between f_0 and p. Thus our model now introduces three parameters b, p and f_0 to be fitted with four experimental quantities: c_{11}, c_{12}, c_{44} and R.

At each temperature, the value of R has been determined from our structural studies [17] while the elastic constants c_{11}, c_{12} and c_{44} have been measured by Haussühl *et al* [5] using sound velocity measurements.

The repulsive contribution W_R to the lattice potential is now the sum of the former Born–Mayer potential plus a 'charge-transfer' W_{CF} term:

$$W_R(r) = W_{CF}(r) + W_{BM}(r). \tag{15}$$

1.3. Results of the three-body interaction model

The TBI model has been established for alkali halides in which the Cauchy discrepancy is small and in which ions have a spherical shape [18]. Complete calculations and a comparison between the RI and TBI model are presented in [18] for these materials.

The situation is somewhat different in alkali cyanides; nevertheless the use of the TBI model described above gives interesting information on the possible influence of the various contributions on the lattice potential during the phase transition process.

Table 3. Values of contributions of the Coulomb potential W_C, the van der Waals potential W_{VDW} and the repulsive potential W_R to the lattice potential W_L in the RI and TBI models.

T (K)	a_0 (Å)	Cauchy discrepancy $c_{12}-c_{44}$	W_C (kcal mol^{-1})	W_{VDW} (kcal mol^{-1})	W_R (kcal mol^{-1})		W_L (kcal mol^{-1})	
					RI	TBI	RI	TBI
293	6.5219	1.0565	−178.205	−15.389	32.563	28.193	−161.481	−165.851
273	6.5154	1.1125	−178.382	−15.935	32.504	27.733	−161.814	−166.584
253	6.5086	1.1635	−178.569	−16.037	32.497	27.355	−162.108	−167.251
233	6.5016	1.2140	−178.761	−16.142	32.520	27.000	−162.384	−167.903
213	6.4943	1.2680	−178.962	−16.253	32.543	26.621	−162.672	−168.585
193	6.4866	1.3290	−179.175	−16.371	32.561	26.180	−162.985	−169.366
173	6.4786	1.4032	−179.396	−16.495	32.533	25.180	−163.358	−170.287
168	6.4766	1.4215	−179.451	−16.526	32.527	25.466	−163.450	−170.511

In table 3, we report the different values of Coulomb potential W_C, the van der Waals potential W_{VDW} and the repulsive potential W_R contributions to the lattice potential W_L in the RI model (without the anisotropic contribution) and in the TBI model. We observe that the introduction of the TBI contribution influences the value (up to 7 kcal mol^{-1}) of the lattice potential and its temperature evolution.

In figure 3, we present the temperature evolution of the lattice potential for KBr and KCN calculated with the RI model together with this potential evolution calculated with the TBI contribution for KCN. In the RI model, the two curves for KBr and KCN lie very close to each other and follow the same temperature evolution. This is mainly due to the similarity of the ionic radii of Br^- and CN^- in a rapidly reorienting configuration. The lattice parameters of the two materials are also little different.

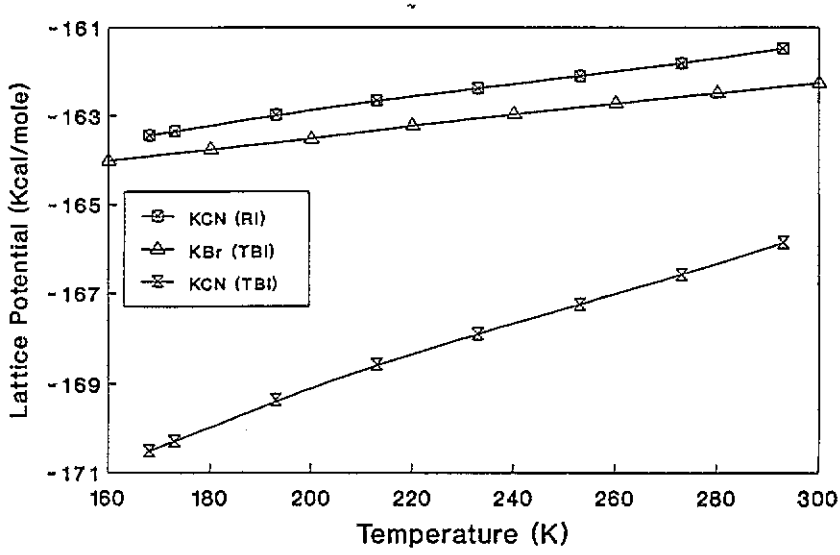

Figure 3. Lattic potentials calculated for KBr with the RI model and for KCN with the RI model and with TBI versus temperature.

We observe an important difference between the RI and TBI model curves for KCN. The RI model assumes that the CN^- molecules are completely disorientated or that the

statistic repartition of CN^- orientation is uniform. This is not correct close to the phase transition temperature. The TBI model takes into account this CN^- orientational effect for each temperature by the introduction into the model of the elastic behaviour of the crystal observed through the Cauchy discrepancy and the bulk modulus values. This anisotropic effect increases with decreasing temperature and the three parameters p, b and f_0 used to take it into account are different from those observed for potassium bromide (table 4).

Table 4. Values at room temperature of parameters p, f_0 and b used in the RI and TBI models for KBr and KCN.

	p (Å)		f_0	b (kcal mol^{-1})	
	TBI	RI	TBI	TBI	RI
KBr	0.368 74	0.367 00	−3.030	5.3097	5.5186
KCN	0.346 37	0.393 59	−306.06	−3.2264	4.9070

For KCN, at room temperature, the overlap parameter p independent of the model chosen has a value comparable with that obtained for alkali bromide [18] while this averaged parameter p largely decreases with increasing temperature when the TBI model is used. It just takes into account the progressive freezing of CN^- dipoles in their preferential orientations ($p = 0.292\,05$ Å *at* 168 K).

The negative pre-exponential factor f_0 in equation (12) has a value two orders of magnitude larger for KCN than for alkali bromide. f_0 strongly increases with decreasing temperature. Nevertheless, figure 4 shows that the 'charge-transfer' effect given by $qq' = (Ze)^2(1 + 6f_0 \exp(-R/p)]^2$ for KCN remains quite constant (around $0.85e^2$) with temperature. This is true also close to the transition temperature.

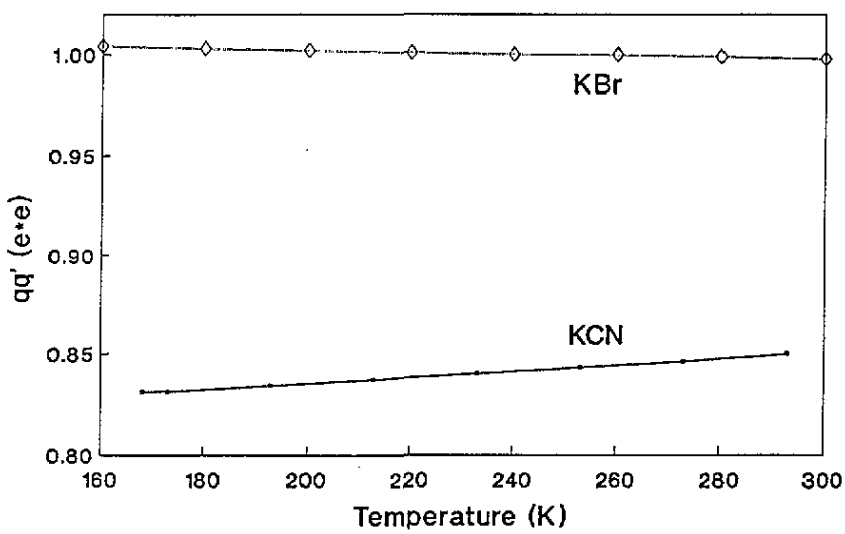

Figure 4. Values of charge transfer qq' versus T obtained by the TBI model for KBr and KCN.

In alkali bromides this charge-transfer effect remains close to unity and shows the good 'ionicity' of these crystals while the charge-transfer effect obtained for KCN is comparable

with the value of the 'ionicity degree' determined by Phillips [19] for AgBr ($0.85e^2$). We know that this compound presents almost the same ionicity as KCN. The charge-transfer value obtained for KCN thus seems to be quite reasonable.

The charge-transfer effect influences the Born–Mayer part of the repulsive contribution and gives a negative parameter b, in order to compensate for the perturbation due to the larger Cauchy discrepancy.

The evolution of Cauchy discrepancy influences p, f_0 and b but has no influence on the ionicity of the K–CN bond. This result is important and shows that the model that we use is macroscopically self-consistent.

1.4. CN pseudo-oriented dipole model

It was interesting to study the lattice potential evolution with temperature considering the CN^- molecule not a single entity but as made up of two identical ions with ionic radii $r_C = r_N = 1.185$ Å [7] separated by a C=N bond whose length d(C–N) equals 1.17 Å, the two ions having a uniform charge $q_C = q_N = -0.5e$.

We thus calculate now the various lattice potentials when all these 'dumbbells' are oriented along one of the three principal directions ⟨001⟩, ⟨110⟩ or ⟨111⟩ of the cubic cell. These directions are not equally probable close to the transition [1]. In none of these configurations has a cubic structure a real meaning. Nevertheless we attempt to calculate a lattice potential using the cubic parameter obtained from x-ray and neutron scattering measurements. In order to keep the averaged pseudo-cubic structure, we assume that the overlap parameter p, found above in the TBI model, takes into account the deformations of the cubic 'cage' surrounding the CN^- independently of its orientation.

The main aim of our calculation is to determine the Coulomb, van der Waals and Born–Mayer contributions to the potential in each of the three CN^- 'orientational configurations'. For this, we calculate for a given 'configuration of orientation' the distances and the angles between the interacting ions K^+, $C^{-0.5}$ and $N^{-0.5}$.

For the Coulomb contribution, these calculations have been made over 1728 unit cells before resulting in a convergence of the series.

For the van der Waals potential, we have introduced the directional value of the CN^- dipole polarizability with a ellipsoidal shape. For each position of the CN^- dumbbell, the polarizability has been calculated using the parallel and perpendicular polarizability values given by Gready *et al* [12].

The repulsive contribution (Born–Mayer type) has been evaluated taking into account the interaction of first and second neighbours according to equation (9).

The parameter b has been adjusted as before from the equilibrium condition (equation (10)).

1.5. Results of pseudo-oriented model

In figure 5, we have reported the temperature evolution of the values of the ⟨001⟩, ⟨110⟩ and ⟨111⟩ pseudo-oriented values of lattice potential. They are combined with the values of the lattice potential obtained previously for the pseudo-cubic TBI model.

At room temperature, of the three possible orientations, the configuration with CN^- molecules oriented along ⟨001⟩ direction represents the lowest potential.

When the temperature decreases, the ⟨111⟩ configuration potential becomes slightly deeper than the ⟨001⟩ potential around 220 K. This means that the ⟨001⟩ and ⟨111⟩ orientations are equally probable at this temperature. This result is in agreement with neutron scattering measurements of the orientation probability of CN^- molecules made by Rowe *et al* [1].

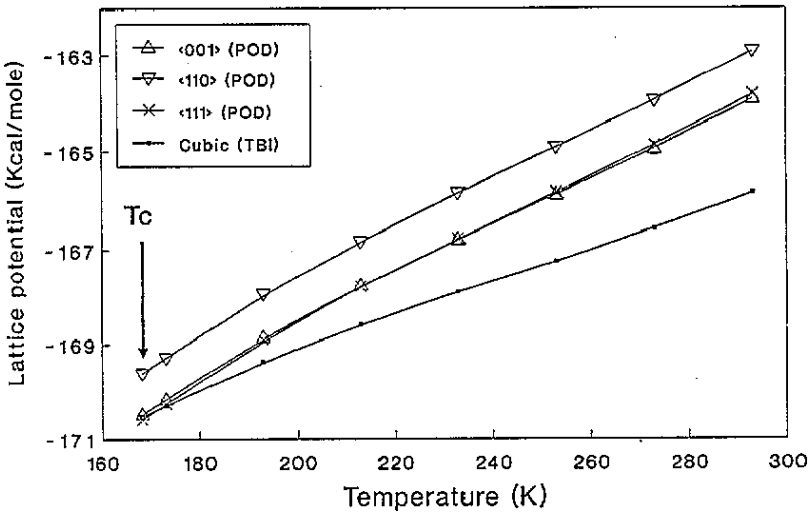

Figure 5. Temperature evolution of potentials for the ⟨001⟩, ⟨111⟩ and ⟨110⟩ POD model together with the values of potential in the TBI model.

Before the experimentally observed transition temperature T_c, the potential obtained from the 'pseudo-cubic' TBI model is deeper than any potential obtained in the POD model. Nevertheless with decreasing temperature the 'oriented' potentials cross the pseudo-cubic potential successively at $T = 107$ K for the ⟨110⟩ orientation, at 156 K for ⟨001⟩ and at 168.5 K for ⟨111⟩.

We note that the experimental transition temperature has been measured at $T_c = 168.3$ K [20], precisely at the temperature, where the ⟨111⟩-oriented potential curve crosses the pseudo-cubic potential line.

Since the work of Bijvoet and Lely [21], we know that below T_c the CN^- dumbbells point towards ⟨110⟩ and not towards ⟨001⟩ or ⟨111⟩ which nevertheless presents above T_c the deepest potentials and the greatest orientation density probabilities. This apparent contradiction needs some discussion which will be given later. We can also observe that the ⟨110⟩-oriented potential crosses the pseudo-cubic potential value at 156 K; this temperature is very close to the temperature at which the elastic constant c_{44} equals zero in KCN [5] ($T = 153$ K).

A rough calculation of the lattice potential has been made below T_c, using the orthorhombic lattice parameters and assuming that the overlap parameter p remains constant and identical with that obtained in the pseudo-cubic TBI model at T_c. The results (table 5) show that the configuration with CN^- dipoles oriented along the ⟨110⟩ direction presents the deepest potential. These rough results indicate only that orthorhombic phases with CN^- oriented along the ⟨001⟩ and ⟨111⟩ directions are not realistic.

Let us recall that the above calculations using the POD model have been made as a guide for interpretation of the experimental results.

2. Discussion

We known from experiment [1] that above T_c the CN^- elastic dipoles point towards the ⟨111⟩ or ⟨001⟩ directions, while below T_c these elastic dipoles are oriented along the ⟨110⟩

direction [21]. Our calculations above and below T_c account for these results. But what is happening at T_c?

Let us try to describe how (before T_c) a CN^- elastic dipole rotates from a ⟨111⟩ direction (which is the most probable orientation in the cubic cell) to another ⟨111⟩ direction.

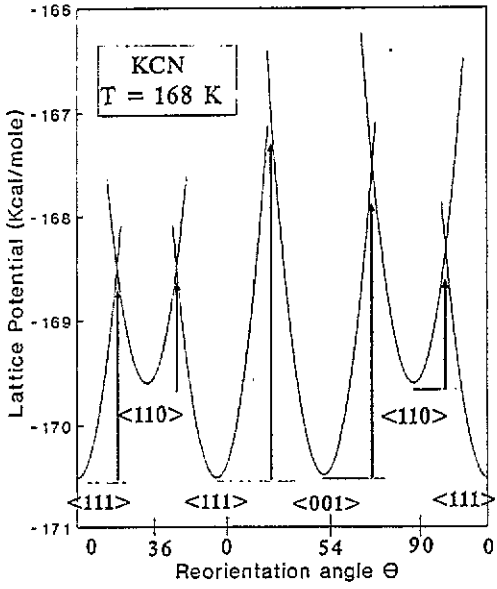

Figure 6. The lattice potential topography above T_c (168 K) versus the angle of rotation for the ⟨110⟩, ⟨111⟩ and ⟨001⟩ orientations of CN^- dumbbells. The shape of the potential between minima has been chosen as a parabolic function of the angle of rotation around each minimum.

Using simple geometrical arguments it is easy to see that, to go from a ⟨111⟩ direction to the closest ⟨001⟩ direction, the dipole must rotate by 54° whereas, from ⟨111⟩ to ⟨110⟩, the rotation is only 36° in the (110) plane. There also exist twice as many ⟨110⟩ directions as ⟨001⟩ directions. Thus, from statistical and geometrical points of view, reorientation from a ⟨111⟩ direction to another ⟨111⟩ orientation is easier by a ⟨110⟩ step than by a ⟨100⟩ step.

Figure 6 reports the lattice potential topography versus angle of rotation for ⟨110⟩, ⟨111⟩ and ⟨001⟩ orientations of CN^- dumbbells just above $T_c = 158$ K. The minima are obtained from our calculations from the POD model, and the shape of the potential between minima has been chosen as a parabolic function of the angle of rotation around each minimum.

Owing to the angular distance between each minimum of the potential, the height of the potential barrier between ⟨111⟩ and ⟨001⟩ minima is higher than between ⟨111⟩ and ⟨110⟩ minima.

The ordering of CN^- dipoles during the phase transition process keeps the ⟨001⟩ cubic direction unchanged with just a contraction of the reticular distance along this direction when passing from the pseudo-cubic cell to the possible orthorhombic cell. When the CN^- molecule occupies one of the three orientations ⟨001⟩, ⟨111⟩ or ⟨110⟩, a simple calculation allows us to evaluate the minimum length of the ⟨001⟩ lattice distance when all ions are in contact along the ⟨001⟩ direction. This distance c_m has to be compared with the cubic lattice

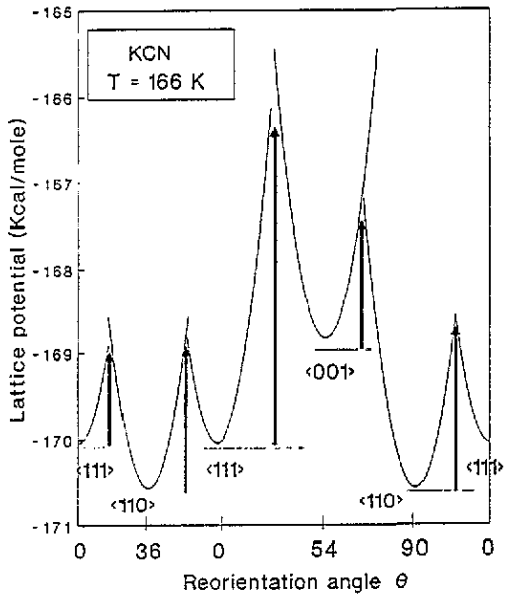

Figure 7. The lattice potential topography below T_c (166 K) versus the angle of rotation for the ⟨110⟩, ⟨111⟩ and ⟨001⟩ orientations of CN^- dumbbells. The shape of the potential between minima has been chosen as a parabolic function of the angle of rotation around each minimum.

parameter at T_c ($a = 6.477$ Å). For the CN^- ⟨001⟩ orientation, $c_m = 2(r_K + r_{CN}) = 6.546$ Å which is greater than a; for the CN^- ⟨111⟩ orientation, $c_m = 2(r_K + r_{CN}/\sqrt{2}) = 5.509$ Å which is less than a; for the CN^- ⟨110⟩ orientation, $c_m = 2r_K + r_C + r_N = 5.376$ Å which is also less than a. This evaluation shows that, just above T_c, a CN^- dipole oriented and stabilized along a ⟨001⟩ direction has not the real space for it. Necessarily the CN^- reorientation through ⟨001⟩ direction induces a shift in the centres of mass of CN^- and K^+ when CN^- is passing by the ⟨001⟩ direction.

Competition between the ⟨111⟩ and ⟨110⟩ orientations is still possible above T_c since steric hindrance of K^+ and CN^- ions leaves space for CN^- orientations in these directions. These two possible orientations allow the crystal to contract in the ⟨001⟩ direction (the E_g-type deformation). Nevertheless the orientation of CN^- in the ⟨110⟩ direction gives the largest possibility for the cell to contract.

Table 5. Values of the lattice potential W_L for three temperatures below T_c using the orthombic lattice parameters measured by the x-ray technique [17].

T	Orthorhombic lattice parameters (Å)			W_L (kcal mol^{-1})		
(K)	a	b	c	⟨001⟩	⟨110⟩	⟨111⟩
168		6.4777		−170.480	−169.609	−170.511
166	4.266	5.103	6.161	−168.835	−170.560	−170.045
130	4.238	5.175	6.144	−168.154	−170.112	−169.441

This E_g-type deformation is thus more favourable to a ⟨110⟩ than to a ⟨111⟩ orientation of the CN^- dipoles and induces the final result of the CN^- ordering process. Below T_c

the potential topography induced by the phase transition is roughly described in figure 7; this topography is deduced from the results given in table 5. We note the change in the potential topography at the phase transition in comparing figure 6 and figure 7. The potential minimum of the the ⟨110⟩ orientation is decreased by about 1 kal mol^{-1} while the potential minima of the ⟨111⟩ and ⟨001⟩ orientations are increased by about 0.5 kcal and 1.5 kcal, respectively, confirming the final orientation of CN^-.

The small difference between the ⟨110⟩ and ⟨111⟩-oriented CN^- potential minima in pure material indicates that any residual stress or defect in the crystal can change the structure of ordered phase just below T_c and explains the appearance of a monoclinic phase in pure KCN when the sample is submitted to thermal cycling or powder grinding [22]. These situations have been described by Michel and Theums [23] as destablization of the orthorhombic structure given the advantage of the antiferroelastic monoclinic phase.

References

[1] Rowe J M, Hinks D G, Price D L, Susman S and Rush J J 1973 *J. Chem. Phys.* **58** 2039
[2] Durand D, Scarvardo do Carmo L C, Anderson A and Lüty F 1980 *Phys. Rev.* B **22** 4005
[3] Lüty F 1981 *Defect on Insulating Crystals* ed V M Turhèvich and K K Shwart (Berlin: Springer) p 61
[4] Wang C H and Satiga S K 1977 *J. Chem. Phys.* **67** 851
[5] Haussühl S, Eckstein J, Recker K and Wallrafen F 1977 *Acta Crystallogr* A **33** 847–9
[6] Cochran W 1971 *Cri. Rev. Solid State Sci.* **2** 1–44
[7] Jenkins H D B and Pratt K F 1976 *J. Inorg. Nucl. Chem.* **38** 1775
[8] Tosi M P 1964 *Solid State Physics* vol 16 (New York: Academic) p 1
[9] Narayan R 1977 *J. Phys. Chem. Solids* **38** 1097
[10] Scott R A and Scheraga H A 1986 *Phys. Status Solidi* b **136** 457
[11] Tessman J R, Kahn A M and Shockley W 1953 *Phys. Rev.* **92** 980
[12] Gready J E, Bacskay G B and Hush N S 1977 *Chem. Phys.* **31** 467
[13] Sysio P A 1969 *Acta Crystallogr.* B **25** 2374
[14] Born M and Mayer J E 1932 *Z. Phys.* **75** 1
[15] Pauling L 1960 *The Nature of the Chemical Bond* (Ithaca, NY: Cornell University Press)
[16] Singh R K, Kumar N and Varshney G V 1986 *Phys. Status Solidi* b **136** 457
[17] Bourson P, Gorczyca G and Durand D 1987 *Cryst. Latt. Defects Amorph. Mater.* **16** 311
[18] Bourson P 1990 *Thesis* University of Metz
[19] Phillips J C 1970 *Rev. Mod. Phys.* **42** 317
[20] Matsuo T, Suga H and Seki S 1968 *Bull. Chem. Soc. Japan* **41** 583
[21] Bijvoet J M and Lely J A 1940 *Rec. Trav. Chem., Pays-Bas* **59** 908
[22] Bourson P, Bouillot J, Soubeyroux J L and Durand D 1991 *Phase Trans.* **31** 277
[23] Michel K H and Theums T 1989 *Phys. Rev.* B **40** 5761